Intercellular Space Is Affected by the Polysialic Acid Content of NCAM

Pinfen Yang, Xinghua Yin, and Urs Rutishauser

Departments of Genetics and Neurosciences, Case Western Reserve University, Cleveland, Ohio 44106

Abstract. We have previously proposed that polysialic acid (PSA), which is attached to NCAM on the cell surface, can serve to regulate a variety of cell–cell interactions. The present study provides evidence that hydrated PSA influences a sufficiently large volume at the cell surface to exert broad steric effects, and that the removal of PSA in fact causes a detectable change in intercellular space. Using F11 neuron/neuroblastoma hybrid cells as a model system, the measured density and size of PSA suggests that a substantial fraction of the space between two apposed cell surface membranes could be sterically influenced by the presence of PSA. Specific enzymatic removal of PSA, which is similar in magnitude to changes that occur in many tissues during normal development, caused about a 25% decrease in the distance between two apposed cells. By contrast, removal of both heparan sulfate and chondroitin sulfate from the cells had no effect on this parameter. It is proposed that such changes in membrane–membrane distance could serve to alter selectively the efficiency of encounter between complementary receptors on apposing cells, and explain at least in part the broad biological influences of PSA.

THE presence of polysaccharides at the surface of animal cells can be attributed to two distinct functional modes: participation in specific recognition phenomena, and contributions to the overall physical/chemical properties of the extracellular environment. Examples of recognition events include sperm–egg interaction (Wassarman, 1987), embryonic compaction (Fenderson et al., 1984) and lectin–carbohydrate binding during leukocyte–endothelial cell interactions (Yednock et al., 1987), and it is likely that a wide variety of such events will be found. The second, which is the subject of the present study, remains less well defined in terms of both its phenomenology and molecular basis. Nevertheless, it is clear that the abundance of membrane-associated carbohydrate in the form of proteoglycans, glycoproteins and glycolipids (see Margolis and Margolis, 1989), represents a major component of cell surface charge and constitutes a hydrated matrix of appreciable size and structural complexity.

A number of observations have led us to propose that a particular cell surface carbohydrate, the polysialic acid moiety (PSA)[1] attached to the neural cell adhesion molecule (NCAM), represents a major glycocalyx component that serves to regulate cell–cell interactions (Rutishauser et al., 1988; Rutishauser, 1989). The PSA content of NCAM is regulated during vertebrate embryogenesis in concert with a variety of developmental events (Chuong and Edelman, 1984; Schlosshauer et al., 1984; Sunshine et al., 1987; Roth et al., 1987; Hekmat et al., 1990; Boisseau et al., 1991), and its presence on NCAM has been postulated to attenuate the function of that molecule's intrinsic adhesive function (Sadoul et al., 1983; Cunningham et al., 1983; Hoffman and Edelman, 1983). However, through the use of a PSA-specific phage endoneuraminidase (endo N), we have demonstrated in vitro that the amount of PSA on NCAM can influence the function not only of NCAM, but of other cell–cell interactions as well (Rutishauser et al., 1988; Acheson and Rutishauser, 1988; Acheson et al., 1991). The effects of endo N on PSA closely resemble the loss of this carbohydrate that occurs naturally in the embryo. Using this enzyme, it has been possible to show in vivo that PSA is a key factor in the establishment of specific innervation patterns of muscle, and that its action in this context is primarily on the L1 adhesion molecule rather than on NCAM (Landmesser et al., 1990). Given the presence of PSA in many nonneural as well as neural tissues (Finne et al., 1987; Roth et al., 1987), this carbohydrate is in a position to influence a wide variety of cell interactions.

There are three fundamentally different mechanisms by which PSA could exert broad effects on cell–cell interaction. In two of them, PSA would act via the NCAM polypeptide, either by generation of some form of transmembrane signal that alters cell biochemistry (Schuch et al., 1989; Doherty et al., 1990), or by affecting a specific association of other receptors with NCAM (Kadmon et al., 1990*a*,*b*). The third mechanism is based on the premise that the unusual physical properties of this very large and abundant linear homopolymer can by themselves affect cell–cell contact (Rutishauser et al., 1988; Rutishauser, 1989).

The purpose of the present study is to test two specific predictions of the third mechanism: that PSA is suitably

1. *Abbreviations used in this paper*: CS, chondroitin sulfate; endo N, endoneuraminidase N; HS, heparan sulfate; NCAM, neural cell adhesion molecule; PSA, polysialic acid.

large and abundant to exert broad steric effects at the cell surface, and that removal of PSA in fact causes a detectable change in the space between two apposed cells. Two lines of experimentation are involved. In the first, we measure the membrane density of NCAM on a cell line that expresses highly sialylated NCAM similar to that found in embryonic brain. The size of the polypeptide and the hydrated polysaccharide is then assessed, and the combined information used to model the steric influence of PSA on the space between two apposed cell membranes. In the second, we determine the relative amount of intercellular space between apposed cells before and after removal of PSA with endo N.

Such studies have not been routine in the study of adhesion molecules, and a number of experimental approaches had to be designed and validated. The results obtained indicate a major role for PSA in regulation of cell–cell apposition and intercellular space, in a manner consistent with the control of receptor–receptor interactions. By contrast, two other major classes of cell surface–associated proteoglycan, heparan sulfate and chondroitin sulfate, were found to have little influence on intercellular space.

Materials and Methods

Cells

The F11 hybrid neuronal cell line was produced by fusion of rat dorsal root ganglion cells with mouse neuroblastoma N18TG2 cells (Platika et al., 1985). Passage 4 F11 cells were obtained from Dr. Lloyd Culp (Case Western Reserve University). F11 cells were grown in DME supplemented with 5% newborn calf serum in a 10% CO_2/humidified air mixture at 37°C (Mugnai et al., 1988). Cells were generally grown to ~80% confluence before harvesting for experiments. All studies were carried out with cells that had undergone less than 12 passages, during which their neuronal properties appear stable (Barletta and Culp, 1990).

Enzymes

PSA was removed from live F11 cells (2×10^6 in 5 ml 50 mg/ml BSA/DMEM) by incubation with 1.5 μg purified endo N (Hallenbeck et al., 1987) at 37°C. Loss of PSA from the cells was confirmed by immunostaining with monoclonal antibody 5A5 and immunoblot analysis. For removal of chondroitin sulfate and heparan sulfate, the cells were treated at 37°C for 2 h with 2.5 U chondroitinase ABC (ICN Biochemicals) and 1.7 U Flavobacterium heparitinase (gift of Dr. Lloyd Culp) in the presence of 1 mM PMSF and 100 nM pepstatin A. The removal of these proteoglycans was evaluated by ^{35}S labeling and gel exclusion chromatography (Vallen et al., 1988) using Sephacryl S300 (Pharmacia Fine Chemicals, Piscataway, NJ).

Antibodies

The 3F4 mouse anti-rat NCAM monoclonal IgG antibody used in these studies was kindly provided by Dr. Richard Akeson (Children's Hospital, Cincinnati, OH) (Akeson et al., 1988). This antibody reacts with an epitope present on both rat and mouse NCAM, as assessed by both SDS-PAGE immunoblots and staining of brain tissue sections (data not shown). PSA was detected using the 5A5 mouse monoclonal IgM (Dodd et al., 1988; Acheson et al., 1991). Polyclonal rabbit anti-mouse NCAM IgG and anti-mouse L1 IgG were prepared against the immunoaffinity-purified antigens, and Fab fragments produced by pepsin digestion.

Measurement of Cell Surface Area

The average total surface area of F11 cells was calculated from two measurements: average spherical area by light microscopy and the degree of membrane convolution as determined from electron micrographs. Although F11 cells display a variety of shapes when attached to tissue culture plates, in suspension they appear as spheres with a moderate range of sizes. The average diameter of F11 cells was determined according to the size distribution of chords measured in bright field photographs (320× magnification) of fixed F11 cells in semi-thick plastic sections after staining with toluidine blue (Coupland, 1968). To assess changes in cell morphology or size caused by fixation and embedding, diameters were also directly measured in phase-contrast micrographs of whole live cells. The average degree of convolution of the plasma membranes of isolated cells was estimated by EM at 5,000× magnification, and expressed as the ratio of total length of membrane projections that were contiguous or noncontiguous in the plane of section, to the circumferential arc passing through the area of observation.

Determination of NCAM Number on Cells

The average number of NCAM molecules expressed on an F11 cell was determined by Scatchard plot analysis of the binding of radioiodinated 3F4 monoclonal anti-NCAM Fab to F11 cell monolayers in 96-well fibronectin-coated tissue culture plates (10^4 cells/well). Cells were cultured 12 h to allow stable attachment, then incubated for 4 h at 4°C with 10–125 ng Fab in 65 μl medium, during which time the cells became nearly spherical but did not detach. Under these conditions the antibody had ready access to essentially the entire cell surface, and equilibrium was established in the binding of Fab to cells. Each condition was analyzed in quadruplicate. Unbound Fab was removed by five rapid (5 s) washes with 200 μl DMEM/20 mM Hepes/1 $mgml^{-1}$ BSA. Less than 5% of the cells were lost from the plates during these washes. The cells were then dissolved in 200 μl 1 M NaOH at 37°C for 1 h and counted for 5 min in a Beckman gamma counter. Nonspecific binding was evaluated by including an excess (7.5 μg) of unlabeled 3F4 Fab during the incubation. Nonspecific values at each Fab concentration were subtracted from total 3F4 binding in preparation of Scatchard plots, and the results analyzed using Ligand software (Munson and Rodbard, 1980; Munson, 1983).

To produce the monoclonal Fab, IgG was treated with immobilized papain (Sigma Chemical Co., St. Louis, MO), undigested antibody and Fc removed by passage through a protein A column (Pierce Chemical Co., Rockford, IL) (Harlow and Lane, 1988), and the Fab concentrated using an Amersham Minicone. Fabs were radioiodinated using solid state lactoperoxidase and glucose oxidase (Sigma Chemical Co.) (Hubbard and Cohn, 1972; David and Reisfeld, 1974). The initial specific radioactivity of 3F4 was 1.14 mCi/mg, and all studies were performed within 30 d after iodination. Over 90% of this radioactivity could be precipitated by 10% cold TCA, and 70% was specifically immunoadsorbed by an excess of either purified rat NCAM or mouse brain membrane vesicles. Nonspecific binding of IgG in these studies was determined using an irrelevant iodinated antibody.

Light Scattering Analysis of NCAM

10 mg of NCAM was purified from E14 chick brain membrane extract by immunoaffinity chromatography (Hoffman et al., 1982) using the mAb 5E (Watanabe et al., 1986; Frelinger and Rutishauser, 1986). PSA was removed from half of this preparation by incubation with endo N (2.5 μg per mg NCAM, 1 h, 37°C). Removal of PSA was confirmed by SDS-PAGE and immunoblot analysis (Acheson et al., 1991) using the 5A5 mAb. The undigested NCAM was exposed to the same incubation conditions. Serial dilutions of both preparations were made in PBS and filtered through Millex-GV 0.22-μm filter units (Millipore Corp., Bedford, MA). The samples were transferred to dust-free test tubes, sealed and kept on ice before being analyzed by a Malvern 4700 system comprising a variable angle light scattering spectrometer (PCS100) interfaced to a K7032 computing correlator. The light source was an Argon laser at 488 nm; NCAM and PSA do not absorb at this wavelength. Protein concentrations were confirmed after the assay by both absorption at OD_{280} and the BCA colorimetric protein assay (Pierce Chemical Co.).

Measurement of Relative Intercellular Space

The space between membranes of apposed F11 cells was assessed by electron microscopic visualization of trapped soluble ferritin (50 mg/ml; Boehringer Mannheim Biochemicals, Indianapolis, IN). These studies were carried out with three cell populations: untreated, treated with endo N to remove PSA, and treated with chondroitinase/heparitinase to remove sulfated proteoglycan. All experiments were carried out in a mixture of polyclonal anti-NCAM (0.5 mg/ml) and anti-L1 (0.1 mg/ml) Fabs, as well as 1 mM EDTA so as to minimize the effects of adhesion molecules on membrane apposition. Cell-cell contact was produced by centrifugation of 10^5 cells in 75 μl onto a 1-mm-thick 1% agar cushion at 1,300 *g* for 3 min in

a BEEM capsule; the cell pellet was then gently overlaid with agar. Thus physical contact of cells was produced by centrifugal force rather than through the affinity of cell surface receptors.

For electron microscopic analysis, the agar-cell pellet-agar sandwiches were cut out of the capsules and fixed with 2.5% glutaraldehyde/0.1 M cacodylate (pH 7.4) for 2.5 h. The samples were then rinsed five times for 15 min with 0.1 M cacodylate (pH 7.4) and postfixed with 2% OsO4/0.1 M cacodylate for 2 h or until the pellets turned black. After rinsing five times for 10 min in water, the pellet was stained overnight with 2% uranyl acetate in water. The sample was dehydrated through a graded acetone/water series and infiltrated with Polybed/812 in acetone. The samples were separated from the capsule ring and incubated for 3 d at 75°C. Three 1-mm^3 blocks were trimmed for each sample and a silver-gold section (~80 mm thick) was collected every 3–4 μm throughout the sample depth, with a total of 20 sections per block. Micrographs were taken at 67,000× magnification at middle positions on each side of each section. Regions of cell-cell contact were scored in terms of linear distance of apposition (as determined using a Bioquant System IV image analysis program), and the total number of ferritin particles contained between the cells within the apposed region.

To control for nonspecific association of ferritin with membranes, F11 cells were attached to fibronectin-coated Aclar disks, exposed for 3 min to the same ferritin solution as above, then rinsed four times in 75 ml PBS within a 20-s period.

Cell-Cell Aggregation Assay

Cells from a 10-cm culture dish at 80% confluence were detached and dispersed by gentle pipetting, and any remaining cell clumps removed by centrifugation at 300 *g* for 1.5 min. The single cells were then pelleted at 450 *g* for 4 min and redispersed in 400 μl ice-cold Hank's Balanced Salts with 2 mg/ml DNAase I, 35 mg/ml BSA, and 1 mM EDTA (HBS), or HBS containing 0.5 mg/ml anti-NCAM Fab and 0.1 mg/ml anti-L1 Fab. After 30 min incubation on ice, 100 μl of cell suspension was diluted with 600 μl HBS at 37°C in scintillation vials, and the vials were rotated at 70 RPM. Duplicate 150-μl aliquots were taken after 0 and 20 min and fixed in 15 ml 1% glutaraldehyde in PBS. The extent of aggregation was assessed by decrease in particle count as determined using a Coulter Counter (Watanabe et al., 1986).

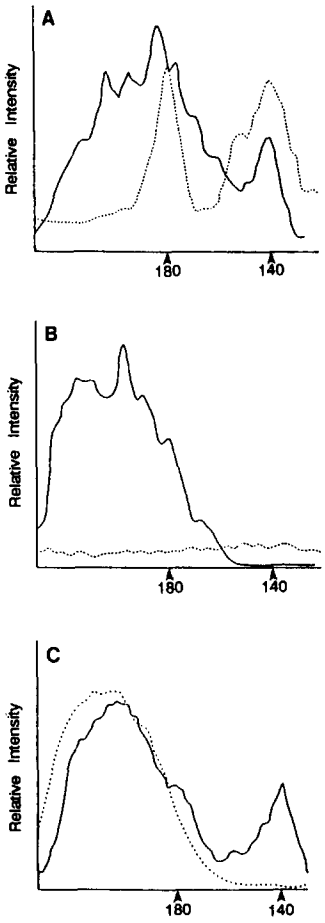

Figure 1. SDS-PAGE immunoblot analysis of NCAM and PSA on F11 cells. (*A*) Extract of F11 cells stained using polyclonal anti-NCAM. (*Solid line*) Without endo N treatment; (*dotted line*) cells treated with endo N before extraction. Note that the endo N treatment reveals the NCAM-140 and NCAM-180 polypeptides. (*B*) Same as in *A* except that the staining was with anti-PSA (5A5 monoclonal). Note that endo N treatment removes all staining for PSA. (*C*) SDS-PAGE of purified embryonic chick brain NCAM after staining for total protein (*solid line*) and PSA (*dotted line*). Note that the overall profiles obtained for NCAM and PSA are similar to those for F11 cells (*solid lines* in *A* and *B*).

Results

A number of new methods or applications were developed for this study, requiring a variety of controls and assumptions. To reserve the Discussion for the biological implications of the findings, the following paragraphs will include, in addition to the data obtained, experimental rationales and evaluation of the methodologies.

Characterization of NCAM on F11 Cells

F11 rat/mouse hybrid cells were chosen for this study because, in contrast with most neuronal cell lines that express NCAM, these hybrids produce NCAM with a high content of PSA. In addition, their interactions with both cells and substrates have been shown to be modulated by the presence of PSA (Acheson et al., 1991). SDS-PAGE immunoblot profiles of the NCAM found on F11 cells are shown in Fig. 1 *A*. Both the low electrophoretic mobility of the NCAM and its susceptibility to endo N is diagnostic of the highly sialylated form of the molecule, with a degree of sialylation approximately comparable to that of NCAM purified from E14 chick brain (Fig. 1 *C*). This result is confirmed by finding that NCAM from F11 cells stains with the PSA-specific 5A5 antibody, and that this staining is abolished by pretreatment of the cells with endo N (Fig. 1 *B*).

Density of NCAM at the Surface of F11 Cells

The 3F4 mAb is directed against an extracellular polypeptide-dependent epitope (Akeson et al., 1988) present on both mouse and rat NCAM (see Materials and Methods). Provided that the antibody has a reasonably high affinity for this epitope, the number of Fabs that bind to F11 cells under saturating conditions should provide an estimate of the total number of NCAM polypeptides present at the cell surface. The Scatchard plots for specific binding of 3F4 Fab to F11 cells are shown in Fig. 2. The data from three such studies with 3F4 fit well to a one epitope model with 4.1 × 10^5 an-

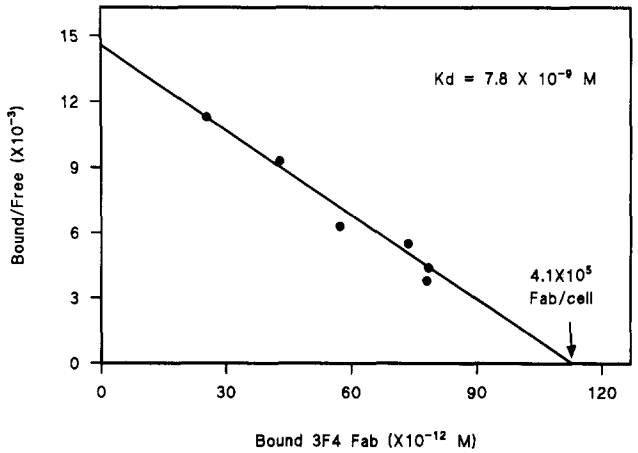

Figure 2. Scatchard analysis of 3F4 Fab binding to F11 cells. See Materials and Methods for details.

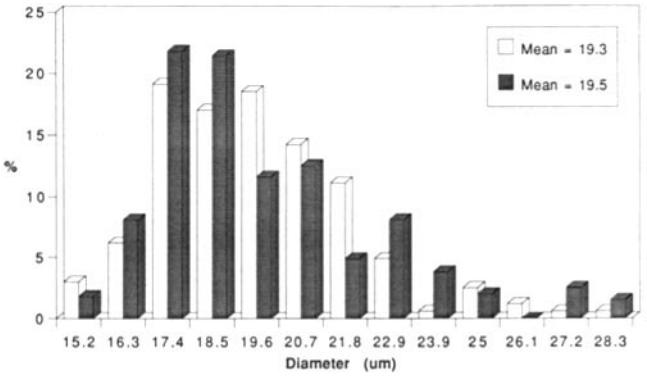

Figure 3. Distribution of F11 cell diameters as calculated from measurements of chords in bright field micrographs of semi-thick plastic sections (*shaded bars*) and as directly measured in phase contrast micrographs of whole live cells (*open bars*). The mean diameter obtained is indicated for the two methods.

tigenic sites per cell and a K_d of 7.8 × 10^{-9} M. The same study was carried out with intact 3F4 IgG and yielded values of 2.9 × 10^5 sites and K_d = 1.9 × 10^{-9} M (data not shown), suggesting that the divalent antibody can bridge NCAMs and thus bind more tightly to the cell; the values obtained with the IgG are similar to those reported previously for a variety of neuroblastoma cell lines (Akeson et al., 1988).

The average diameter of cells was determined both from the distribution of chords in a section through a plastic-embedded cell pellet (Coupland, 1968), and by direct measurement of whole live cells (Fig. 3). The two methods gave the same result, indicating that the fixation and embedding procedures did not drastically alter the morphology of the cells. Electron micrographs of thin sections of F11 cells indicated that a factor of 3.6 is required to correct spherical areas for convolutions of the surface membrane (see Materials and Methods). From these values, the average membrane surface area of a rounded-up F11 cell was calculated to be 4,200 μm^2. Thus, with 4.1 × 10^5 NCAMs/cell, and assuming a uniform distribution of NCAM in the membrane of free cells, each 100 × 100 nm square area of membrane contains on average about one NCAM polypeptide.

Light Scattering Analysis of NCAM with and without PSA

The estimation of the excluded volume of PSA on NCAM is subject to two complexities, the large amount of water associated with the carbohydrate and the tendency of NCAM to aggregate in solution. The first led to the use of dynamic light scattering to estimate the size of the hydrated particle. These measurements were carried out both on purified embryonic brain NCAM (Fig. 4), which has a PSA content similar to that of NCAM on F11 cells (Fig. 1), and on the same preparation treated with endo N to remove PSA (as confirmed by SDS-PAGE immunoblots, Fig. 4). The second complexity is that at the concentrations required for light scattering (0.2–1 mg/ml), purified NCAM exists in solution as multimers produced via specific homophilic and/or

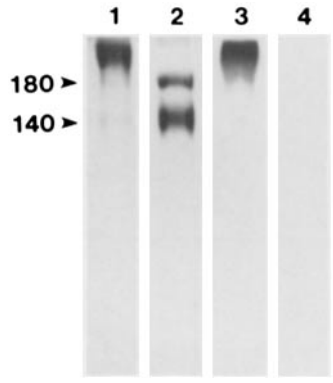

Figure 4. SDS-PAGE of purified chick embryonic NCAM used in light scattering analyses. (Lane *1*) Untreated NCAM stained for total protein; (lane *2*) endo N-treated NCAM stained for total protein; (lane *3*) untreated NCAM stained with 5A5 anti-PSA; (lane *4*) endo N-treated NCAM stained with 5A5 anti-PSA.

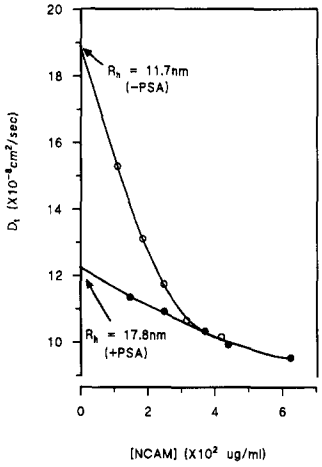

Figure 5. Translational diffusion coefficients (D_t) measured by dynamic light scattering as a function of NCAM concentration. (*Solid points*) NCAM with intact PSA; (*open points*) NCAM treated with endo N (see Fig. 4). Extrapolation to zero NCAM concentration gave values of $D_t°$ = 12.3 × 10^{-8} and 18.7 × 10^{-8} cm^2/s for NCAM + PSA and NCAM − PSA, respectively. The radii of hydration (*Rh*) for the two forms of NCAM were calculated from $D_t°$ using the Stokes-Einstein relationship.

Table I. Dynamic Light Scattering Analysis of NCAM with and without PSA

	Experiment		
	1	2	3
R_h (+PSA)(nm)	19.0	15.2	17.8
R_h (−PSA)(nm)	14.1	10.8	11.7
R_h ratio (+/−)	1.4	1.4	1.5
Volume ratio (+/−)	2.8	2.8	3.4

Translational diffusion coefficients (D_t) were measured at 22°C for both NCAM(+PSA) and NCAM(−PSA) solutions after extrapolation to zero concentration. The radii of hydration (R_h, in nm) were calculated from $D_t°$ using the Stokes-Einstein relationship.

Table II. Density of Ferritin Particles between Apposed Membranes of F11 Cells

	Experiment					
	1		2		3	
PSA	+	−	+	−	+	+
CS and HS*	+	+	+	+	+	−
EM Sample						
A	14.1	10.2	12.0	9.7	13.1	12.9
B	13.2	8.0	12.0	9.7	12.7	12.3
C	13.7	9.0	11.9	9.7	12.1	12.3
Avg	13.7	9.1	12.0	9.7	12.6	12.5

Values represent the average number of ferritin particles per micron of apposed membrane as observed in electron micrographs (See Fig. 6). The number of fields scored were 50 in experiments 1 and 3, and 75 in experiment 2. In experiments 1 and 2, values with and without PSA are significantly different using the Scheffe F-test ($p < 0.05$). The values with and without HS and CS are not significantly different.

* CS, chondroitin sulfate; HS, heparan sulfate.

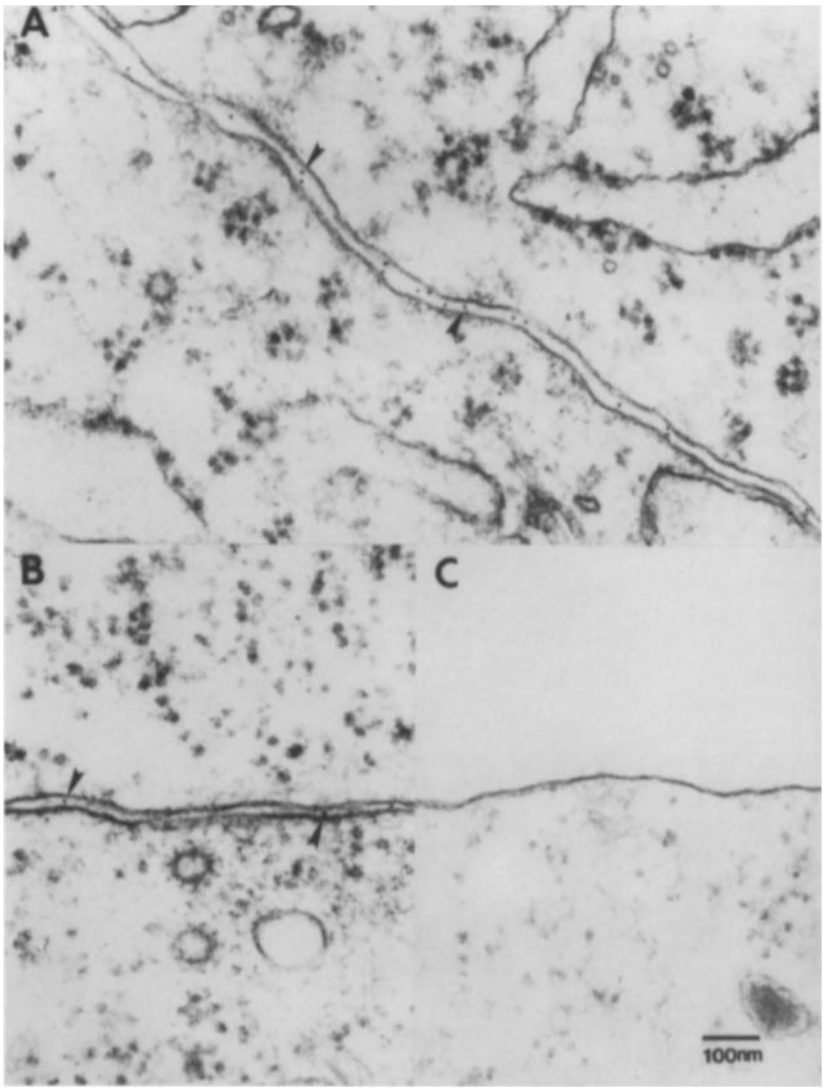

Figure 6. Typical electron micrographs used to quantitate trapped ferritin particles (*arrowheads*) in apposed regions of F11 cell membranes without (*A*) and with (*B*) endo N treatment. In the small sample represented by individual micrographs, the membrane–membrane distances and densities of ferritin varied widely, but in a large sample the removal of PSA resulted in a significant decrease in trapped ferritin as summarized in Table II. All samples represent cells pelleted in the presence of anti-NCAM, anti-L1 and EDTA to inhibit cell-cell adhesion (see Fig. 7 and Table III). *C* illustrates that ferritin was not associated with unapposed membranes after brief washing (see Materials and Methods).

nonspecific hydrophobic interactions (Hoffman et al., 1982; Hall and Rutishauser, 1987; Becker et al., 1991). As detergents were not effective in preventing this aggregation, PBS was chosen as the solvent since its use avoided the need to resolve scattering due to detergent micelles from that of the glycoprotein. Since the degree of aggregation of soluble NCAM is only slightly if at all affected by the degree of polysialylation (Hall and Rutishauser, 1987), it was possible to use these results to determine the ratio of the hydrated volumes for the molecule with and without PSA.

In three independent experiments, of which Fig. 5 presents representative data, the ratio of hydrated volumes for intact and endo N-treated NCAM was consistently about threefold (Table I). The absolute values obtained for R_h were greater than would be predicted for a single polypeptide of a bent rod of ~4 nm by 40 nm (Hall and Rutishauser, 1987; Becker et al., 1989). These values confirm that NCAM is not a monomer in solution (Hoffman et al., 1982; Hall and Rutishauser, 1987). The variability in the values of R_h in the three experiments probably reflects differences in the degree of aggregation and polysialylation in different NCAM preparations as well as experimental errors associated with the light scattering measurements. While aggregate size does not appear to change significantly with desialylation of NCAM (Hoffman et al., 1982; Hall and Rutishauser, 1987), it may be noted that any such increase would result in an underestimate of the hydrated volume of PSA.

Measurement of Relative Intercellular Spaces

The measurement of intercellular spaces in a cell pellet must be carried out visually because the total extracellular volume is dominated by spaces produced by imperfect packing of the cells. However, the method best suited to a visual assay, transmission EM of plastic sections, involves sample dehydration and consequently poor preservation of the heavily hydrated extracellular environment.

One approach to this problem is to introduce a visible particle at known concentration into the extracellular environment, and then to count these particles in defined regions of cell–cell contact (Table II). The particle must be sufficiently electron dense for unambiguous identification, yet not so large as to impede membrane–membrane contact or sediment significantly during pelleting of the cells. It must also be present at sufficient concentration to provide statistically significant numbers in small volumes and have no detectable

Table III. Inhibition of F11 Cell Aggregation by Polyclonal Fabs against NCAM and L1

Fab	−	+	+
PSA	+	+	−
Aggregation*	29 ± 9	4 ± 4	4 ± 3

All assays were carried out in the presence of 1 mM EDTA. Data represent the mean of four values from each of two independent experiments.
* Aggregation is expressed as the percent decrease in particle number after rotation at 70 RPM for 20 min at 37°C.

affinity for any membrane-associated component. These criteria were fulfilled by a 50 mg/ml solution of ferritin, and typical sections through cells pelleted in ferritin are shown in Fig. 6. Ferritin was found not to have a significant affinity for the surface of isolated F11 cells (Fig. 6).

As will be discussed, an important goal of this study is to distinguish between PSA acting as a physical element in impeding the overall apposition of membranes, versus its possible direct effects on the intrinsic binding properties of adhesion receptors in general, and of NCAM in particular. For this reason, all studies have been carried out with cells exposed to three potent adhesion-blocking agents: polyclonal Fabs against NCAM and L1, and EDTA. The effectiveness of these agents with F11 cells was assessed in terms of both short-term cell aggregation assays and the overall appearance of the cell pellets. As shown in Table III, the natural aggregation of F11 cells in suspension (Acheson et al., 1991) was completely blocked by these agents. When F11 cells were brought into contact by centrifugation into BEEM capsules, the dense clustering of cells normally produced by their natural adhesiveness was absent when the cells had been treated by the Fab/EDTA mixture (Fig. 7). In both the aggregation assay and the pellets, the effectiveness of the inhibitors was not decreased when PSA was removed from the cells by endo N (Table III and Fig. 7).

The next step in the analysis was to prepare F11 cells from which PSA or sulfated proteoglycans had been specifically removed. As shown in Figs. 1 and 8, endo N treatment was effective in converting the NCAM on F11 cells to the low sialic acid form. Similarly, a mixture of chondroitinase and heparatinase was effective in the removal of sulfated proteoglycans associated with F11 cells (Fig. 9). While little sulfated carbohydrate remained on the cells, the amount of PSA was not reduced detectably by the mixture of these two enzymes (Fig. 8).

The measurement of trapped ferritin between apposed membranes of F11 cells with and without PSA and sulfated proteoglycans, is summarized in Table II. The results, obtained in triplicate in two independent experiments, are that the removal of PSA causes a consistent and significant decrease (25%) in the number of ferritin molecules per micrometer of apposed membrane. By contrast, removal of sulfated proteoglycans is without effect on this parameter (Table II). In all cases the ferritin particles appeared to be randomly distributed not only along the regions of apposed membranes, but also with respect to the gap between the two bilayers. The latter suggests that the soluble ferritin is not physically excluded from the intercellular space.

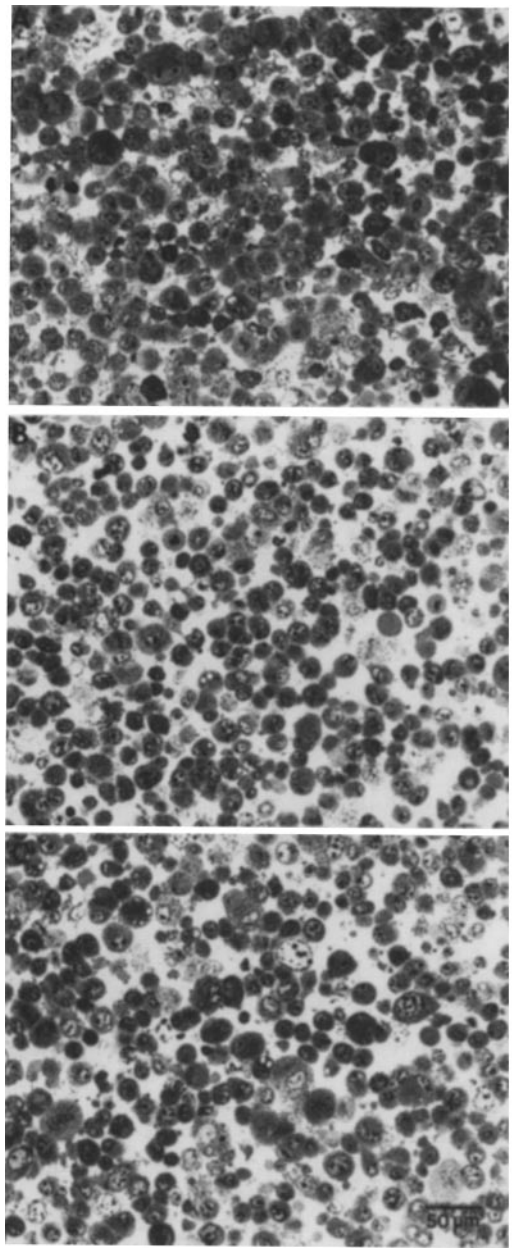

Figure 7. Bright field micrographs of F11 cells in pellets used to measure trapped ferritin. (*A*) Cells without addition of Fabs. (*B*) Cells pelleted in the presence of anti-NCAM Fab, anti-L1 Fab and EDTA. (*C*) Cells pretreated with endo N and pelleted with Fabs and EDTA. Note that the natural adhesiveness of F11 cells causes formation of dense cell clumps in *A*, and that this aggregation is absent with addition of the Fabs and EDTA, both with (*B*) and without (*A*) endo N treatment. All samples were sectioned from the same plastic blocks used for electron microscopy.

Discussion

The present studies provide direct evidence that the abundance of NCAM at the cell surface, and the unusual physical properties of the PSA attached to NCAM, can affect the closeness of membrane–membrane contact. These observations are consistent with the proposal that the regulation of cell surface PSA on NCAM during development can serve to regulate the efficiency of encounter between receptors on apposing cells. The following discussion evaluates the basis for these conclusions and their possible implications for regulation of specific cell–cell interactions.

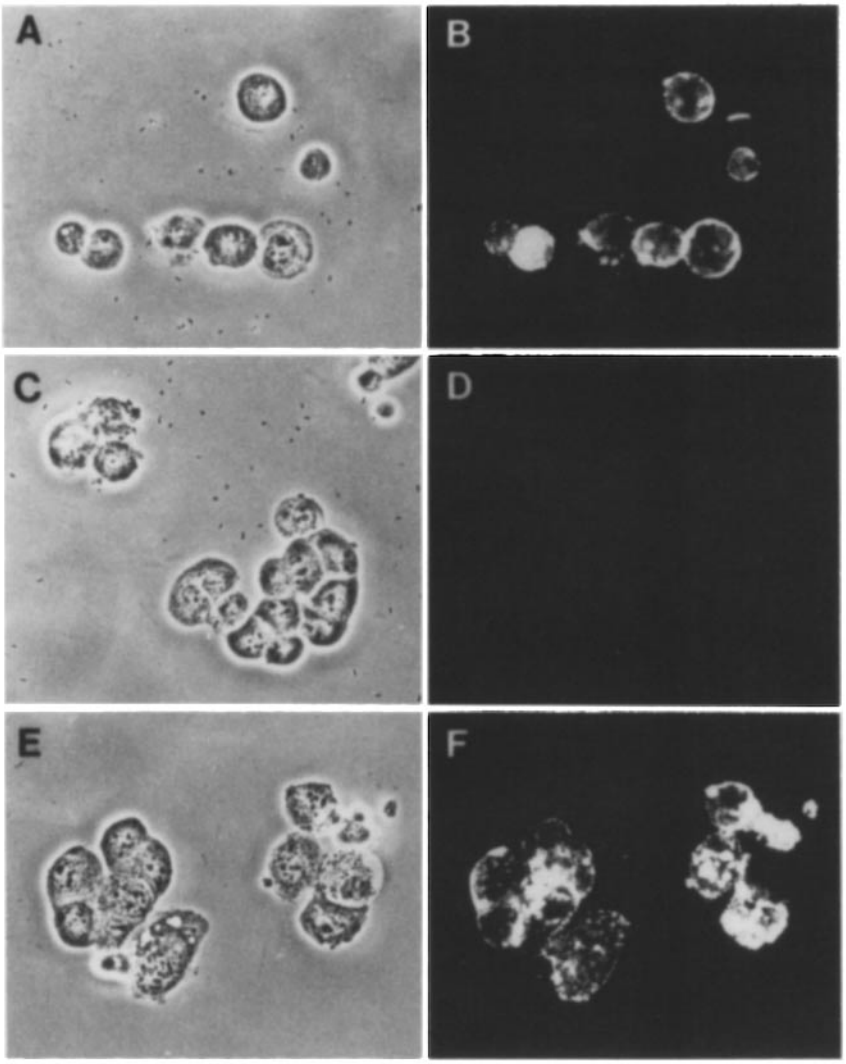

Figure 8. Phase-contrast and anti-PSA immunofluorescence micrographs of F11 cells (*A* and *B*) untreated, (*C* and *D*) treated with endo N, and (*E* and *F*) treated with both heparatinase and chondroitinase. Whereas endo N completely eliminates staining for PSA, there was no significant loss of PSA staining with prior removal of chondroitin sulfate and heparan sulfate (see Fig. 9).

Gram-negative bacteria are known to utilize PSA (as colominic acid) as a surface coat (Vimr et al., 1984), and it has been shown that PSA on NCAM can in fact form an unusually thick coating on Wilms kidney tumor cells (Zuber and Roth, 1990; Roth and Zuber, 1990). In the present study, the goal has been to determine whether PSA also functions as a physical coating of a cell with neuronal properties.

The first question is whether PSA on F11 neuronal cells is sufficiently large and abundant to constitute such a physical presence. Fig. 10 depicts a scale representation of two apposed cell surface membranes, each bearing NCAM at the density indicated by our Fab-binding study. The size of the NCAM polypeptide in this schematic is derived from electron micrographs (Hall and Rutishauser, 1987; Becker et al., 1989), and the excluded volume of PSA represents the fact that the hydrated volume of NCAM with PSA is about three times that of the polypeptide. The fact that integral surface proteins such as NCAM can rotate rapidly in the plane of the membrane (Cherry, 1979), is assumed to increase the influence of the molecule's excluded volume during the relatively slow process of cell–cell contact. Moreover, it is important to remember that NCAM represents only a small fraction of total cell surface protein, with other membrane components in sum also occupying a considerable volume. Thus it would appear that the surface of an F11 cell is a crowded environment in which the addition or removal of a bulky carbohydrate could have a pronounced effect on cell–cell encounters.

Ultimately the critical test of the model is whether intercellular space is actually altered by differences in the PSA content of NCAM. For reasons described in the Introduction, it is difficult to obtain a direct measure of this parameter. Thus we have devised a method based on quantitation of the amount of a visible and inert tracer (ferritin) that is trapped between apposed membranes. As mentioned above, these studies were carried out under conditions where the cells have been rendered nonadhesive. This manipulation was necessary in order to exclude the alternative that PSA removal was reducing intercellular space by directly enhancing the binding properties of adhesion molecules.

The reproducible decrease in the amount of ferritin trapped between apposed membranes after PSA removal argues strongly that the amount of intercellular space has decreased. Since this result was obtained for a constant area of apposition, the affected parameter is likely to be the distance between the two bilayers. Two other surface-associated proteoglycans that are easily detected and removed, namely those containing heparan sulfate and chondroitin sulfate, did

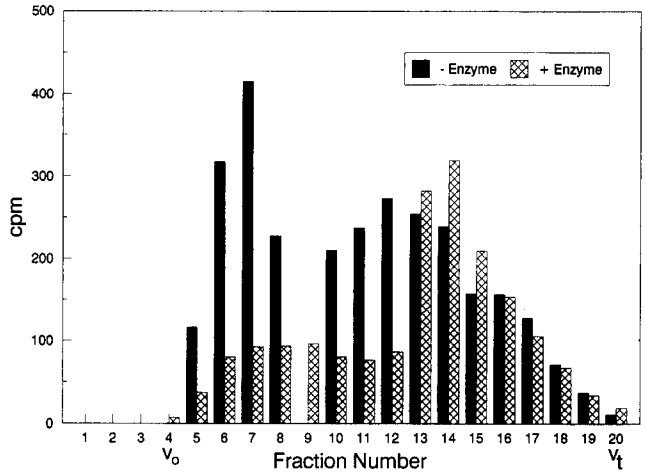

Figure 9. Sephacryl S300 gel filtration analysis of F11 cell extracts demonstrating the presence of high molecular weight sulfated proteoglycans with these cells (*solid bars*; fraction 9 was lost) and their removal by treatment with heparatinase and chondroitinase (*hatched bars*). See Methods for details.

not appear to influence intercellular space to a measurable extent. It remains to be determined, however, whether still other large cell surface components (for example, membrane-bound hyaluronic acid) might be able to influence this parameter as well.

For a variety of reasons, such as leakage of some tracer and the presence of other molecules in the intercellular space, it is difficult to estimate volumes and distances from the number of ferritin particles counted. Nevertheless, it is valuable to speculate on the magnitude of the changes involved. A change of about one-quarter in membrane–membrane distance is not so great as to dwarf the physical dimensions of large cell surface proteins such as the NCAM, L1, cadherin and integrin adhesion receptors. Nevertheless, the binding activities of these molecules are often associated with specific regions along an extended multi-domain structure. Thus any shift in distances of this magnitude would be expected to alter the efficiency of receptor–receptor interaction. For purposes of illustration, Fig. 11 depicts an array of hypothetical receptor pairs on apposing membranes. Assuming an intercellular distance of ~50 nm (the extracellular domain of an NCAM-like receptor extends up to ~30 nm), the removal of PSA would reduce this dimension by over 10 nm. Considering that an Ig domain is ~4 nm long, the nature of the overall interaction would be likely to change. However, as individual receptors differ in their length, flexibility and location of binding sites, some might be able to compensate for the change or even be activated by the increase in membrane distance.

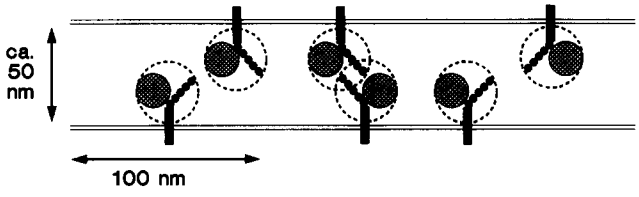

Figure 10. Scale representation of the interaction between two cell membranes, each bearing NCAM at the density measured for F11 cells (see text). A random distribution of NCAM on the cell surface is assumed. The size and bent rod shape of the NCAM polypeptide with five 4-nm Ig domains was derived from electron micrographs (Hall and Rutishauser, 1987; Becker et al., 1989). The size of the PSA (*hatched circles*) attached to the fifth domain reflects the increase in radius of hydration of the polysialylated molecule (Table I). The dashed circle around each NCAM represents the ability of the integral membrane proteins to rotate rapidly in the plane of the biolayer (Cherry, 1979). The approximate intercellular distance shown reflects the dimensions of receptor pairs that span the two membranes.

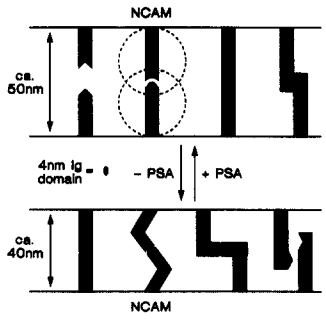

Figure 11. Schematic representation of the variety of influences that the observed changes in intercellular space could have on interactions between different types of receptor pairs. For NCAM, partial reduction of binding occurs. For some receptors, such as L1, the presence of PSA appears to reduce sharply the efficiency of interaction (*left*). For others (*right*), the opposite effect could occur, while long and flexible receptors (*middle*) might not be affected at all.

This situation is consistent with the hypothesis that cell-cell interactions are more influenced by the rate of receptor encounter than by the intrinsic affinities of the receptors themselves (Lawrence and Springer, 1991; Williams, 1991). By hindering membrane contact, PSA decreases the rate of binding among receptors on apposing cells, without affecting the intrinsic binding properties of those receptors. Thus the constraints of membrane–membrane contact should, along with restrictions in the movement and positioning of receptors in a bilayer, be considered as major parameters in specifying the nature of cell interactions.

As outlined in the Introduction, there are at least two alternative mechanisms by which PSA could affect cell interactions receptors other than NCAM. With respect to hypotheses that NCAM might generate transmembrane signals (Schuch et al., 1989) that could be affected by PSA (Doherty et al., 1990), it should be noted that at least some of PSA's ability to alter membrane–membrane adhesion can be demonstrated with brain membrane vesicles and reconstituted vesicles containing purified NCAM (Hoffman and Edelman, 1983; Rutishauser et al., 1985). Thus the effects of PSA on adhesion are apparent in the absence of most cytoplasmic and cytoskeletal elements. The possibility remains that PSA removal might activate an auxiliary function for NCAM, as in the proposed "assisted homophilic" function of L1 (Kadmon et al., 1990*a*,*b*). However, the present studies were deliberately carried out under conditions in which adhesion molecule function (including both NCAM and L1) was inhibited, and thus the observed changes in intercellular distances are unlikely to reflect such effects.

In summary, the present study provides an important confirmation of the proposal that at least some of PSA's function reflects an effect on overall membrane–membrane and consequently receptor–receptor interaction. In this mode, PSA apparently can act independently of the intrinsic binding properties of those receptors, including those of NCAM

itself. For F11 cells, the ability of PSA to exert a global physical presence provides a simple explanation for the otherwise surprising observation that PSA can affect cell adhesion to tissue culture matrices as well as to other cells, and that these phenomena are not influenced by antibodies that block NCAM-mediated adhesion (Acheson et al., 1991). Most importantly, the present findings should facilitate our fundamental understanding of the ability of PSA regulation in vivo to influence axon growth and sprouting (Landmesser et al., 1988, 1990), and assist in the interpretation of its presence in specific regions of other embryonic tissues, such as muscle and kidney. In this respect, however, it is also clear that improved methods will need to be developed to measure directly membrane–membrane distances in intact tissues.

The authors wish to thank Drs. James Jamieson and Lynn Sobey for their advice and assistance with the light scattering studies, Dr. Lloyd Culp for advice, David Starke for assistance with proteoglycan analyses, Dr. Ruth Siegal for advice on the determination of receptor number, and Dr. Vance Lemmon for review of the manuscript.

The study was funded in part by National Institutes of Health grants HD18369 and EY06107.

Received for publication 23 September 1991 and in revised form 23 December 1991.

References

Acheson, A., and U. Rutishauser. 1988. NCAM regulates cell contact-mediated changes in choline acetyltransferase activity of embryonic chick sympathetic neurons. *J. Cell Biol.* 106:479–486.

Acheson, A., J. L. Sunshine, and U. Rutishauser. 1991. NCAM polysialic acid can regulate both cell-cell and cell-substrate interactions. *J. Cell Biol.* 114:143–153.

Akeson, R. A., J. R. Wujek, S. Roe, S. L. Warren, and S. J. Small. 1988. Smooth muscle cells transiently express NCAM. *Mol. Br. Res.* 4:107–120.

Barletta, E., and L. A. Culp. 1990. Clonal segregation of multiple and overlapping matrix adhesive responses in dorsal root neuronal derivative cells. *J. Cell. Physiol.* 143:263–278.

Becker, J. W., H. P. Erickson, S. Hoffman, B. A. Cunningham, and G. M. Edelman. 1989. Topology of cell adhesion molecules. *Proc. Natl. Acad. Sci. USA.* 86:1088–1092.

Boisseau, S., J. Nedelec, V. Poirier, G. Rougon, and M. Simonneau. 1991. Analysis of high PSA N-CAM expression during mammalian spinal cord and peripheral nervous system development. *Development (Camb.).* 112:69–82.

Cherry, R. J. 1979. Rotational and lateral diffusion of membrane proteins. *Biochim. Biophys. Acta.* 559:289–327.

Chuong, C.-M., and G. M. Edelman. 1984. Alterations in neural cell adhesion molecules during development of different regions of the nervous system. *J. Neurosci.* 4(9):2354–2368.

Coupland, R. E. 1968. Determining size and distribution of sizes of spherical bodies such as chromaffin granules in tissue sections. *Nature (Lond.).* 217:384–388.

Cunningham, B. A., S. Hoffman, U. Rutishauser, J. J. Hemperly, and G. M. Edelman. 1983. Molecular topography of the neural cell adhesion molecule N-CAM: Surface orientation and location of sialic acid-rich and binding regions. *Proc. Natl. Acad. Sci. USA.* 80:3116–3120.

David, G. S., and R. A. Reisfeld. 1974. Protein iodination with solid state lactoperoxidase. *Biochemistry* 13:1014–1021.

Dodd, J., S. B. Morton, D. Karagogeos, M. Yamamoto, and T. M. Jessell. 1988. Spatial regulation of axonal glycoprotein expression on subsets of embryonic spinal neurons. *Neuron.* 1:105–116.

Doherty, P., J. Cohen, and F. S. Walsh. 1990. Neurite outgrowth in response to transfected N-CAM changes during development and is modulated by polysialic acid. *Neuron.* 5:209–219.

Fenderson, B. A., U. Zehavi, and S. I. Hakomori. 1984. A multivalent lacto-N-fucopentose III-lysyllysine conjugate decompacts preimplantation mouse embryos, while the free oligo-saccharide is ineffective. *J. Exp. Med.* 160: 1591–1596.

Finne, J., D. Bitter-Suermann, C. Goridis, and U. Finne. 1987. An IgG monoclonal antibody to group B menningococci cross-reacts with developmentally regulated polysialic acid units of glycoproteins in neural and extraneural tissues. *J. Immunol.* 138:4402–4407.

Frelinger, A. L., and U. Rutishauser. 1986. Topography of NCAM structural and functional determinants. II. Placement of monoclonal antibody epitopes. *J. Cell Biol.* 103:1729–1737.

Hall, A. K., and U. Rutishauser. 1987. Visualization of neural cell adhesion molecule by electron microscopy. *J. Cell Biol.* 104:1579–1586.

Hallenbeck, P. C., E. R. Vimr, F. Yu, B. Bassler, and F. A. Troy. 1987. Purification and properties of a bacteriophage-induced Endo-N-acetylneuraminidase specific for Poly-a-2,8-sialosyl carbohydrate units. *J. Biol. Chem.* 262(8):3553–3561.

Harlow, E., and D. Lane. 1988. Antibodies: A Laboratory Manual. Cold Spring Harbor Laboratory Press. 628–630.

Hekmat, A., D. Bitter-Suermann, and M. Schachner. 1990. Immunocytological localization of the highly polysialylated form of the neural cell adhesion molecule during development of the murine cerebellar cortex. *J. Comp. Neurol.* 291:457–467.

Hoffman, S., B. C. Sorkin, P.C. White, R. Brackenbury, R. Mailhammer, U. Rutishauser, B. A. Cunningham, and G. M. Edelman. 1982. Chemical characterization of a neural cell adhesion molecule (N-CAM) purified from embryonic brain membranes. *J. Biol. Chem.* 257:7720–7729.

Hoffman, S., and G. M. Edelman. 1983. Kinetics of homophilic binding by embryonic and adult forms of the neural cell adhesion molecule. *Proc. Natl. Acad. Sci. USA.* 80:5762–5766.

Hubbard, A. L., and Z. A. Cohn. 1972. The enzymatic iodination of the red cell membrane. *J. Cell Biol.* 55:390–405.

Kadmon, G., A. Kowitz, P. Altevogt, and M. Schachner. 1990*a*. The neural cell adhesion molecule N-CAM enhances L1-dependent cell-cell interactions. *J. Cell Biol.* 110:193–208.

Kadmon, G., A. Kowitz, P. Altevogt, and M. Schachner. 1990*b*. Functional cooperation between the neural adhesion molecules L1 and N-CAM is carbohydrate dependent. *J. Cell Biol.* 110:209–218.

Landmesser, L., L. Dahm, K. Schultz, and U. Rutishauser. 1988. Distinct roles for adhesion molecules during innervation of embryonic chick muscle. *Dev. Biol.* 103:645–670.

Landmesser, L., L. Dahm, J. Tang, and U. Rutishauser. 1990. Polysialic acid as a regulator of intramuscular nerve branching during embryonic development. *Neuron.* 4:655–667.

Lawrence, M. B., and T. A. Springer. 1991. Leukocytes roll on a selectin at physiologic flow rates: distinction from and prerequisite for adhesion through integrins. *Cell.* 65:859–873.

Macklin, W. B., and C. L. Weill. 1985. Appearance of myelin proteins during development in the chick central nervous system. *Dev. Neurosci.* 7:170–178.

Margolis, R. U., and R. K. Margolis, editors. 1989. Neurobiology of Glycoconjugates. Plenum Press, New York. 1–453.

Mugnai, G., K. Lewandowska, and L. A. Culp. 1988. Multiple and alternative adhesive responses on defined substrata of immortalized dorsal root neuron hybrid cell line. *Eur. J. Cell Biol.* 46:352–361.

Munson, P. J. 1983. Ligand: a computerized analysis of ligand binding data. *Methods Enzymol.* 92:543–576.

Munson, P. J., and D. Rodbard. 1980. Ligand: a versatile computerized approach for characterization of ligand-binding systems. *Anal. Biochem.* 107:220–239.

Platika, D., M. H. Boulos, L. Baizer, and M. C. Fishman. 1985. Neuronal traits of clonal cell lines derived by fusion of dorsal root ganglia neurons with neuroblastoma cells. *Proc. Natl. Acad. Sci. USA.* 82:3499–3503.

Roth, J., and C. Zuber. 1990. Immunoelectron microscopic investigation of surface coat of Wilms tumor cells. *Lab. Invest.* 62:55–60.

Roth, J., D. J. Taatjes, D. Bitter-Suermann, and J. Finne. 1987. Polysialic acid units are spatially and temporally expressed in developing postnatal rat kidney. *Proc. Natl. Acad. Sci. USA.* 84:1969–1973.

Rutishauser, U. 1989. Polysialic acid as a regulator of cell interactions. *In* Neurobiology of Glycoconjugates. R. U. Margolis and R. K. Margolis, editors. Plenum Publishing, New York. 367–382.

Rutishauser, U., M. Watanabe, J. Silver, F. A. Troy, and E. R. Vimr. 1985. Specific alteration of NCAM-mediated cell adhesion by an endoneuraminidase. *J. Cell Biol.* 101:1842–1849.

Rutishauser, U., A. Acheson, A. K. Hall, D. M. Mann, and J. Sunshine. 1988. The neural cell adhesion molecule (NCAM) as a regulator of cell-cell interactions. *Science (Wash. DC).* 240:53–57.

Sadoul, R., M. Hirn, H. Deagostini-Bazin, G. Rougon, and C. Goridis. 1983. Adult and embryonic mouse neural cell adhesion molecules have different binding properties. *Nature (Lond.).* 304:349.

Schlosshauer, B., U. Schwartz, and U. Rutishauser. 1984. Topological distribution of different forms of NCAM in the developing chick visual system. *Nature (Lond.).* 310:141–143.

Schuch, U., M. J. Lohse, and M. Schachner. 1989. Neural cell adhesion molecules influence second messenger systems. *Neuron.* 3:13–20.

Sunshine, J., K. Balak, U. Rutishauser, and M. Jacobson. 1987. Changes in neural cell adhesion molecule (NCAM) structure during vertebrate neural development. *Proc. Natl. Acad. Sci. USA.* 84:5986–5990.

Williams. A. F. 1991. Cellular interactions: out of equilibrium. *Nature (Lond.).* 352:473–474.

Vallen, E. A., K. A. Eldridge, and L. A. Culp. 1988. Heparan sulfate proteoglycans in the substratum adhesion sites of human neuroblastoma cells: modulation of affinity binding to fibronectin. *J. Cell Physiol.* 135:200–212.

Vimr, E. R., R. D. McCoy, H. F. Vollger, N. C. Wilkison, and F. A. Troy. 1984. Use of prokaryotic-derived probes to identify poly(sialic acid) in neonatal membranes. *Proc. Natl. Acad. Sci. USA.* 81:1971–1975.

Wassarman, P. M. 1987. The biology and chemistry of fertilization. *Science*

(Wash. DC). 235:553–560.

Watanabe, M., A. L. Frelinger, and U. Rutishauser. 1986. Topology of NCAM structural and functional determinants. I. Classification of monoclonal antibody epitopes. *J. Cell Biol.* 103:1721–1727.

Yednock, T. A., E. C. Butcher, L. M. Stoolman, and S. D. Rosen. 1987. Receptors involved in lymphocyte homing: relationship between a carbohydrate-binding receptor and the MEL-14 antigen. *J. Cell Biol.* 104:725–731.

Zuber, C., and J. Roth. 1990. The relationship of polysialic acid and the neural cell adhesion molecule N-CAM in Wilms tumor and their subcellular distributions. *Eur. J. Cell Biol.* 51:313–321.